# Single-Layer Model of the Hexagonal Boron Nitride Nanomesh on the Rh(111) Surface

Robert Laskowski, Peter Blaha, Thomas Gallauner, and Karlheinz Schwarz
*Institute of Materials Chemistry, Technische Universität Wien, Getreidemarkt 9/165TC, A-1060 Vienna, Austria*
(Received 14 November 2006; published 7 March 2007)

An alternative model of the hexagonal boron nitride (*h*-BN) on nanomesh on the Rh(111) surface is presented. It explains the observed ultraviolet photoelectron spectroscopy spectra and reproduces experimental STM images introducing, instead of two, only one strongly corrugated layer of *h*-BN covering the whole Rh surface. In order to optimize the geometry of the BN layer we calculate the forces by density functional theory and analyze the interactions in the system. The final geometry is a result of a competition between BN-metal attraction or repulsion and elastic properties of the isolated *h*-BN layer. The calculated bonding energy is around 0.33 eV per BN molecule with a corrugation close to 0.55 Å.

DOI: 10.1103/PhysRevLett.98.106802 PACS numbers: 73.20.At, 68.37.Ef, 73.22.−f

The search for nanostructured new materials, in particular, when formed by self-assembly, is of great importance and thus a very active field of research. Recently, such a self-assembling structure was detected when borazine is thermally decomposed on a Rh(111) surface [1]. Boron nitride forms a highly regular *h*-BN/Rh(111) nanomesh with a periodicity of about 3.2 nanometers. A hexagonal unit cell consisting of a $12 \times 12$ Rh substrate, on which a $13 \times 13$ *h*-BN forms, was deduced from LEED patterns, surface x-ray diffraction [2], and STM pictures. A periodic hole structure of about 2 nm diameter was observed within this unit cell. Based on the STM images and on ultraviolet photoelectron spectroscopy (UPS) data, which showed a splitting of the BN-$\sigma$ bands, an atomic model was suggested which consists of two (partially incomplete) boron nitride (BN) layers. The functionality of this nanomesh was demonstrated by decoration with $C_{60}$ molecules [1]. Recently an almost identical structure has been found on the Ru(0001) surface [3], whereas on Pd(111) [4], Pd(110) [5], and Pt(111) some kind of moiré pattern appears but on Ni(111) [6–11] and Cu(111) [12] a simple $1 \times 1$ *h*-BN monolayer forms. While the difference between the Ni or Cu systems and all others can easily be understood in terms of lattice mismatch between *h*-BN and the metal surface, the underlying mechanism of the nanomesh formation just on Rh (and Ru) and its atomic structure are not understood so far. The present two layer model becomes quite unrealistic when one considers that many broken B-N bonds occur in the partially incomplete layers. Test calculations have shown that the resulting dangling bonds cause a high energy penalty making such structures highly unstable.

In this Letter we present an alternative atomic model for the *h*-BN/Rh(111) nanomesh, provide an understanding of the *h*-BN interaction with transition metal (TM) surfaces, and explain the different structures found on various TM. The proposed structure consists of only a single layer of *h*-BN, which, however, is highly corrugated. The theoretically predicted corrugation is consistent with both, the observed splitting of the BN-$\sigma$ bands as well as with the experimental STM images [1]. It is essential to know which structural model of the nanomesh is correct, because otherwise one cannot understand or modify its functionality.

The best studied *h*-BN/TM system is *h*-BN/Ni(111) [6–9], which consists of an epitaxial $1 \times 1$ BN monolayer. Theoretical calculations [10,11] found that a stable monolayer of *h*-BN only forms when B is in the fcc or hcp hollow site and N is on top of Ni [see Fig. 1 of Ref. [10]; we will call this (fcc, top) or (hcp, top) further on]. The BN layer is not flat but is slightly buckled, with B about 0.1 Å closer to the Ni surface than N. Direct *ab initio* calculations of the *h*-BN/Rh(111) nanomesh are much more difficult due to the large number of atoms (144 Rh and 338 B and N atoms/layer) and the metallic character. Therefore, we employed an *ab initio* derived force field for the structural optimization, which is described below. The final structure has been checked by full density functional theory (DFT) calculations.

All *ab initio* calculations have been carried out within DFT using the method of augmented plane waves plus local orbitals APW + LO as implemented in the Wien2k package [13,14]. For the exchange-correlation potential the recent Wu-Cohen–generalized gradient approximation (GGA) has been used [15], as it gives in general a better description of solids than the more common PBE-GGA [16]. The surface calculations have been performed with a slab geometry with seven layers of Rh, covered on both sides by BN and separated by sufficient vacuum of approximately 6.5 Å thickness. The Brillouin zone was sampled with a $14 \times 14 \times 1$ mesh of *k* points. The APW + LO basis set quality was determined by $RK_{max} = 6.0$ with muffin-tin radii of 1.06 and 0.71 Å for Rh and N or B, respectively. The convergence criteria for self-consistent force calculations has been set to 10 meV/Å.

In order to derive a force field but also to understand the dominant interactions we made the following steps: in step 1 we strain BN by 8% to match the Rh(111) lattice, a model that can be represented by a $1 \times 1$ unit cell as in Ref. [10]. In step 2 we calculated by DFT the forces acting on a flat BN layer in the (fcc, top) position as a function of the BN-Rh distance. Figure 1 shows the important result, namely, that for all distances N is repelled from (positive force), but

 © 2007 The American Physical Society

B is attracted (negative force) to the surface. For BN closer than the equilibrium distance (2.2 Å), the N repulsion is stronger than the B attraction, whereas for larger distances the B attraction dominates. This is rather surprising, since so far all commonly accepted models considered the direct TM-N bond as primary source of attraction. These forces also explain why the BN surfaces want to be buckled with B closer to the TM than N, and invalidate the former interpretation that *h*-BN on Ni(111) is buckled due to the slight compression of the *h*-BN layer [8,17]. By analyzing the electronic structure we find that for N, both the bonding and antibonding N $p_z$–Rh $d_{z^2}$ states are occupied, whereas for B the corresponding antibonding states are at higher energy and thus empty. This causes the differences in the forces between B and N. In contrast to Rh, late TMs like Ni have much weaker bonds to *h*-BN due to the higher *d*-band filling and thus a larger occupation of the antibonding states. When we allow the Rh surface to relax, the Rh surface atoms initially follow the BN displacement, trying to keep the Rh-BN distance constant (Fig. 1, dashed line). Similarly to Ni(111) we also find for Rh(111) that BN is repelled when N is on another high-symmetry position like the hcp or fcc hollow site, irrespectively where B sits.

In step 3 we generalize these findings by laterally displacing BN with respect to the Rh surface at a given distance $z$. The resulting forces for $z = 2.17$ Å above Rh (slightly smaller than equilibrium) and 2.57 Å ("far" away from the surface) are displayed in Fig. 2. We can see that N is always repelled and B always attracted, but the N repulsion is weakest near the top site, but strongest near fcc, while for B the opposite happens (except for large $z$, where hcp is less attractive than top). Note that these forces change almost stepwise along the $xy$ directions, i.e., small displacements from the high-symmetry positions do not affect the force, but once the displacements are large, a rather strong variation of the resulting forces sets in. This has important consequences for the proposed model discussed later. In total we determined the forces between Rh(111) and strained *h*-BN positioned at various $xyz$ positions on a $10 \times 10 \times 8$ grid in the unit cell. This defines the anharmonic Rh-BN force field, which cannot be described by two effective force constants between Rh-N and Rh-B, since these interactions are highly anharmonic and position dependent. We have verified that the Rh-BN forces described above do not change significantly between strained and unstrained BN by additional $3 \times 3$ supercell calculations, where the BN distance was partly changed to its optimal value.

In step 4 we study how the initially flat and isolated *h*-BN monolayer deforms due to the Rh-BN interactions. In order to describe the vertical elastic response, we calculated the forces when either B or N are displaced perpendicular to the hexagonal plane. The main effects are already included when a small buckling of the B relative to the N subnet is introduced in a $1 \times 1$ unit cell. It turns out that such a deformation is quite harmonic and nearly the same for B and N, with a force constant equal to 14.6 eV/Å$^2$. When a $2 \times 2$ supercell is considered, but only one of the N or B atoms is displaced, all first and second nearest neighbors of the displaced atom remain at their initial positions. The induced forces remain harmonic, but strongly depend on the displaced atom. For B the response is practically the same as for the $1 \times 1$ deformation and the second neighbor B atoms have almost zero force. For N, however, the restoring force is almost halved. Moreover, the forces induced on the first neighbor B atoms are the same as in the $1 \times 1$ cell, but the forces induced on the second neighbors N have considerable values. From these facts we infer a N-N repulsive interaction, which is due to a polarization effect mediated by different deformations of the BN bonds. As this NN repulsion decreases the force acting on N it will enhance the curvature of the *h*-BN monolayer. Its effective force constant is close to 6.8 eV/Å$^2$ (acting only on N). We have also verified that the influence of the Rh surface on the elastic parameters of *h*-BN is small. For that, we used the force field to deter-

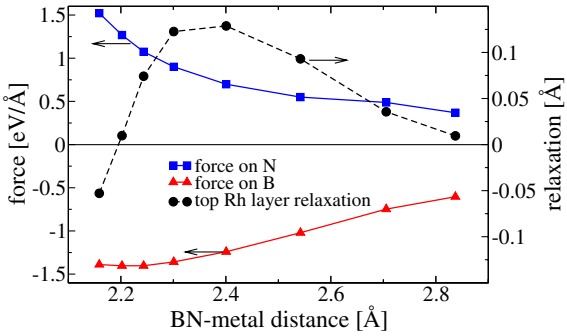


FIG. 1 (color online). The $z$ dependence of the force acting on B and N atoms of a flat *h*-BN monolayer in (fcc, top) configuration and relaxation of the first metal layer. Note that at equilibrium the *h*-BN layer is buckled with B and N at 2.04 Å and 2.18 Å away from the metal surface, respectively.

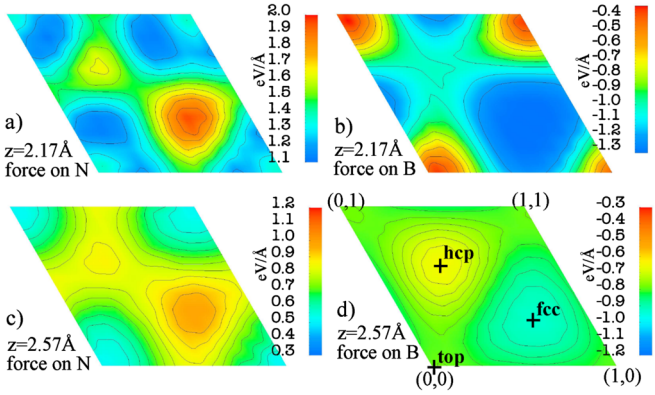


FIG. 2 (color online). Surface map of the $z$ force component acting on N and B atoms. The calculations are performed with a flat BN layer placed 2.17 Å [(a), (b)] and 2.57 Å [(c), (d)] from the surface. When N is positioned at $(x, y, z)$, B is at $(x + 2/3, y + 1/3, z)$.

mine the buckling of $h$-BN/Rh(111) in (fcc, top) $1 \times 1$ geometry. The *ab initio* and the force field values are within 10% the same.

Step 5 considers a lateral displacement of the B subnet versus the N subnet within the hexagonal plane. It leads to a rather large force constant of about 48.6 eV/Å$^2$, reflecting the fact that laterally BN is rather stiff and a change in bond length costs quite some energy. Therefore, lateral deformations are of less importance but they were also included in our model.

In the final step we simulated the full nanomesh using a DFT derived force field, which consists of a combination of the harmonic BN force constants for stretching (step 5) and buckling (step 4) of BN and the forces between both, B and N, and the Rh surface. The latter is interpolated from the forces obtained in step 3 (as indicated in Fig. 1 and 2), taking the B and N coordinates with respect to the underlying $1 \times 1$ Rh unit cell. We put a $13 \times 13$ $h$-BN monolayer on top of a $12 \times 12$ Rh(111) slab and performed a full geometry optimization of the B and N atomic positions neglecting any possible relaxations of the surface Rh atoms. Later on we will briefly discuss the effects of this approximation.

The optimized structure is presented in Fig. 3, where the upper panel [Fig. 3(a)] shows a map of the $z$ coordinate of N atoms in a $3 \times 3$ nanomesh unit cell, while the lower panel [Fig. 3(b)] displays a ball and stick model of one unit cell of the $h$-BN/Rh(111) nanomesh with one layer of Rh atoms. The BN layer is apparently strongly corrugated and the distance between N and the metal surface varies from 2.17 Å to 2.72 Å. One can clearly distinguish two regions: first, a rather flat area where BN is close to the metal, located around the origin of the unit cell, i.e., a region where B and N atoms are close to their optimal (fcc, top) positions with respect to the underlying Rh atoms. We will call this the "low" region, which covers about 70% of the nanomesh unit cell. When the B and N atoms cannot keep their optimal positions above Rh due to the lattice mismatch, they are repelled from the surface and a second region builds up, where BN is placed further away from the metal surface (the "high" region). Within this high region we can distinguish two slightly different heights of BN, a higher and a lower one. The difference between these regions is that around (1/3, 2/3) B and N atoms are located close to (hcp, fcc) positions, whereas near (2/3, 1/3) they occupy (top, hcp) sites. The difference in height can be understood from the forces in Fig. 2, where BN on (hcp, fcc) have the weakest attraction and strongest repulsion, respectively. When the difference between the two peaks is neglected the layer may look like having a sixfold symmetry axis. Considering this difference may give the impression of a threefold symmetry axis, but actually only a mirror plane normal to (110) remains (see the different left-right connections of the two maxima in Fig. 3). Such a symmetry breaking has already been observed in STM images of the BN nanomesh [1]. Another important observation is that the nanomesh structure has an almost stepwise corrugation. The transition between low and high regions is relatively abrupt. This has important consequences for experimental measurements, as one can expect signals related to low and high regions with a ratio 70:30, but almost no signal from the transition area.

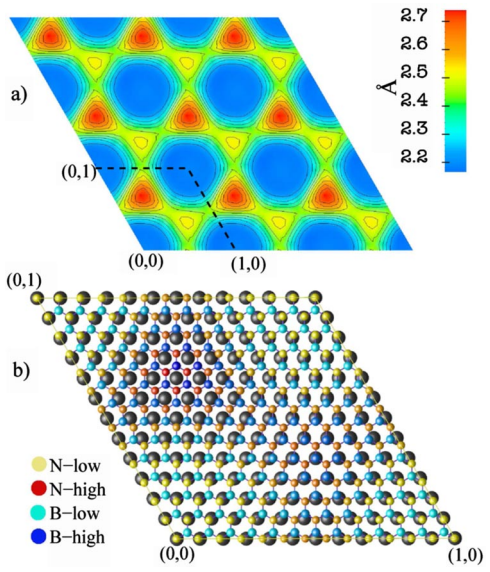


FIG. 3 (color online). The atomic structure of the $h$-BN/Rh(111) nanomesh. (a) Contour map of the $z$ coordinate of N atoms in the $3 \times 3$ nanomesh unit cell. (b) Ball and stick model of the $h$-BN/Rh(111) nanomesh unit cell (with just one metal layer). Colors indicate the height of the B and N atoms.

The amplitude of the "low-high" corrugation of the BN layer is about 0.55 Å. This value is very close to the corrugation observed in STM images by Corso *et al.* [1], while in any two layer model the distance between BN sheets should be about 3 Å, i.e., comparable to the interlayer distance of bulk $h$-BN.

In order to further support our model, we have calculated the electronic structure for $1 \times 1$ $h$-BN/Rh(111) with BN located above Rh as found in the low (fcc, top) and high (hcp, fcc) regions of the nanomesh. The density of states (DOS) presented in Fig. 4 shows a shift of the N $p_{x,y}$ derived DOS by about 1 eV which compares very well with the experimentally observed splitting of the $\sigma$ bands (Fig. 4

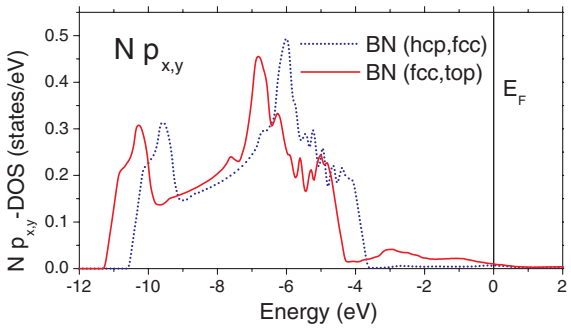


FIG. 4 (color online). N-$p_{,y}$ density of states calculated for low (N-top, B-fcc) and high (N-fcc, B-hcp configurations) regions.

from Corso *et al.* [1] ). The low energy feature stems from BN at the bonding (low) sites and the corresponding shift is due to an additional charge transfer of $0.1e^-$ from B to N, while the upper peak corresponds to BN further away from the surface at the high region (almost bulk $h$-BN). Moreover, the intensity ratio of the $\sigma_1$ and $\sigma_2$ peaks in their spectra suggest the area of the two kinds of BN species to be about 2.5. This value is again very close to the ratio of low and high regions observed in our model and confirms that the experimental $\sigma_1$ peak stems from BN closely attached to Rh, while $\sigma_2$ is related to loosely bound BN. We should point out that this $\sigma$-band splitting is almost saturated at a bond length difference of 0.55 Å between the low and high BN above the metal surface, where a larger corrugation would hardly affect it. Thus the slightly different maxima at $(1/3, 2/3)$ and $(2/3, 1/3)$ of our nanomesh structure would hardly be visible in UPS spectroscopy.

The estimated value of the binding energy of the corrugated BN layer to the metal surface is roughly a sum of the binding of BN in the low and high regions (weighted by the corresponding areas) and the energy cost due to the BN layer deformation. The binding energy in low configuration with respect to the strained and flat BN is equal to 0.49 eV. For the high region the BN is repelled from the surface with a negative binding energy of $-0.04$ eV. The total binding energy is estimated to be about 0.33 eV per BN molecule. According to our calculations a commensurate BN configuration (fcc, top) with stretched BN bonds would not lead to any binding, since the BN-Rh attraction (0.49 eV) is compensated by the BN stretching ($-0.50$ eV). Since the binding energy between $h$-BN and Ru is even stronger (0.85 eV), we expect that the Ru nanomesh is even more stable, while the epitaxial $h$-BN/Ni(111) system binds only with 0.19 eV. Note that these binding energies provide trends, but depend strongly on the exchange correlation functional where LDA gives larger, PBE smaller binding [11].

By analyzing the forces acting on the metal atoms as a function of BN position we expect that the top metal layer will not be completely flat, since Rh follows partly the BN corrugation. The Rh surface should be corrugated by about 0.1 Å (see Fig. 1). Preliminary calculations using the DFT linear scaling pseudopotential code OPENMX [18] confirm both the small Rh corrugation and the structure of the corrugated BN nanomesh.

To conclude, we presented an alternative structural model of the BN nanomesh on the Rh(111) surface. It consists of a single BN layer with a $12 \times 12$ Rh and $13 \times 13$ BN periodicity to accommodate the lattice mismatch, but the BN layer is highly corrugated due to the differences in chemical bonding of BN above different Rh sites. The structure is unique and quite different from common strain relieve patterns or dislocation networks, since the lateral BN distances remain almost unchanged throughout the nanomesh. Our model disagrees with the one originally proposed by Corso *et al.* [1], but can explain the experimentally observed $\sigma$ band splitting and seems to be consistent with very recent STM images [19]. Finally, our model is not only applicable to other $h$-BN/TM systems like Ru (much stronger interaction) or Pt (much weaker interaction), where it can explain or verify and predict the corresponding structures, but most likely the method can be generalized to other interfaces where the lattice mismatch and the resulting big nanostructures do not allow a straightforward *ab initio* simulation.

This work was supported by the EU (No. FP6-013817) and Austrian Research Fund (SFB Aurora No. F1108). We would like to thank J. Osterwalder and T. Greber for many stimulating discussions.

[1] M. Corso, W. Auwärter, M. Muntwiler, A. Tamai, T. Greber, and J. Osterwalder, Science **303**, 217 (2004).
[2] O. Bunk *et al.*, Surf. Sci. **601**, L7 (2007).
[3] A. Goriachko, Y. He, M. Knapp, and H. Over, Langmuir (to be published).
[4] M. Morscher, M. Corso, T. Greber, and J. Osterwalder, Surf. Sci. **600**, 3280 (2006).
[5] M. Corso, T. Greber, and J. Osterwalder, Surf. Sci. **577**, L78 (2005).
[6] A. Nagashima, N. Tejima, Y. Gamou, T. Kawai, and C. Oshima, Phys. Rev. Lett. **75**, 3918 (1995).
[7] A. Nagashima, N. Tejima, Y. Gamou, T. Kawai, and C. Oshima, Phys. Rev. B **51**, 4606 (1995).
[8] W. Auwärter, T. J. Kreutz, T. Greber, and J. Osterwalder, Surf. Sci. **429**, 229 (1999).
[9] A. B. Preobrajenski, A. S. Vinogradov, and N. Mårtensson, Phys. Rev. B **70**, 165404 (2004).
[10] G. B. Grad, P. Blaha, K. Schwarz, W. Auwärter, and T. Greber, Phys. Rev. B **68**, 085404 (2003).
[11] M. N. Huda and L. Kleinman, Phys. Rev. B **74**, 075418 (2006).
[12] A. B. Preobrajenski, A. S. Vinogradov, and N. Mårtensson, Surf. Sci. **582**, 21 (2005).
[13] P. Blaha, K. Schwarz, G. K. H. Madsen, D. Kvasnicka, and J. Luitz, *WIEN2k, An Augmented Plane Wave Plus Local Orbitals Program for Calculating Crystal Properties* (Vienna University of Technology, Vienna, Austria, 2001), ISBN 3-9501031-1-2.
[14] G. K. H. Madsen, P. Blaha, K. Schwarz, E. Sjöstedt, and L. Nordström, Phys. Rev. B **64**, 195134 (2001).
[15] Z. Wu and R. E. Cohen, Phys. Rev. B **73**, 235116 (2006).
[16] J. P. Perdew, K. Burke, and M. Ernzerhof, Phys. Rev. Lett. **77**, 3865 (1996).
[17] W. Auwärter, H. U. Suter, H. Sachdev, and T. Greber, Chem. Mater. **16**, 343 (2004).
[18] T. Ozaki, Phys. Rev. B **74**, 245101 (2006).
[19] S. Berner, M. Corso, R. Widmer, O. Groening, R. Laskowski, P. Blaha, K. Schwarz, A. Goriachko, H. Over, S. Gsell, M. Schreck, H. Sachdev, T. Greber, and J. Osterwalder, Angew. Chem.-Int. Edit. (to be published).